

# Intramolecular Electron Density Redistribution upon Hydrogen Bond Formation in the Anion Methyl Orange at the Water/1,2-Dichloroethane Interface Probed by Phase Interference Second Harmonic Generation

Juliette Rinuy,<sup>[a]</sup> Alexis Piron,<sup>[a]</sup> Pierre François Brevet,<sup>[a]</sup> Mireille Blanchard-Desce,<sup>[b]</sup> and Hubert H. Girault\*<sup>[a]</sup>

**Abstract:** Surface second harmonic generation (SSHG) studies of the azobenzene derivative *p*-dimethylaminoazobenzene sulfonate, often referred as Methyl Orange (MO), at the neat water/1,2-dichloroethane (DCE) interface is reported. The two forms of the anionic MO dye, which are usually observed in bulk solution, with one form being hydrogen bonded to a water molecule through the azo nitrogens (MO/H<sub>2</sub>O) and the other form not being hydrogen bonded (MO) have also been observed at the water/DCE interface. Their equilibrium constant has been compared with the corresponding bulk solution

and found to be identical. The adsorption equilibrium of the two forms has been determined and the Gibbs energy of adsorption measured to be  $-30 \text{ kJ mol}^{-1}$  for both forms. From a light polarisation analysis of the SH signal, the angle of orientation of the MO transition dipole moment was found to be  $34 \pm 2^\circ$  for MO and  $43 \pm 2^\circ$  for MO/H<sub>2</sub>O under the assumption of a

Dirac delta function for the angle distribution, a difference explained by the different solvation properties of the two forms. Furthermore, the wavelength dependence analysis of these data revealed an interference pattern resulting from the electronic density redistribution within the hydrated anionic form occurring upon the formation of the hydrogen bond with a water molecule. This interference pattern was clearly evidenced with the use of another dye at the interface in order to define a phase reference to both forms of Methyl Orange.

**Keywords:** electronic structure • hydrogen bonds • liquid/liquid interfaces • Methyl Orange • nonlinear optics

## Introduction

Many fundamental biological reactions involve species adsorption at membrane surfaces, for instance before the transfer of the species across the membrane into or out of the cell. In this respect, liquid/liquid interfaces can be used as simple models to study fundamental processes in biological membranes. In the past adsorption processes at these interfaces have been extensively studied, notably by surface tension measurements.<sup>[1]</sup> More recently, the interfacial environment of adsorbed species has been investigated by optical means in order to get a molecular picture of the solute–solvent interactions at the liquid/liquid interface. To achieve interfacial sensitivity with the optical signal, the geometry of

total internal reflection (TIR) was used, whereby the incident wave impinges onto the interface from the medium with the highest refractive index. The transmitted evanescent wave intensity then decreases with a typical value for the characteristic penetration depth in the nanometer range, of about 150 nm for example at the water–DCE interface with an angle of incidence of  $67^\circ$ . In many cases, this interfacial sensitivity is not sufficient enough to dwarf the response from the two adjacent bulk phases; furthermore dedicated properties of the fluorescent probes, such as surfactant behavior, have to be met in order to record true interfacial processes.<sup>[2,3]</sup> Despite these drawbacks, interfacial phenomena such as photoinduced electron transfer reactions have been reported.<sup>[4]</sup> In this context, the use of nonlinear optics as a tool to probe surfaces and interfaces has rapidly been recognized as an efficient technique. Indeed, nonlinear processes of even order are forbidden in the electric dipole approximation in centrosymmetric media like liquids and thus signals only arise from the surface or the interface where the centrosymmetry is broken.<sup>[5,6]</sup> Surface second harmonic generation (SSHG) is a first order nonlinear process whereby two photons at the fundamental frequency  $\omega$  are converted into one photon at the harmonic frequency  $2\omega$ . Despite the weakness of the SH

[a] Prof. H. H. Girault, J. Rinuy, A. Piron, Dr. P. F. Brevet  
Laboratoire d'Electrochimie  
Ecole Polytechnique Fédérale de Lausanne  
1015 Lausanne (Switzerland)  
Fax: (+41) 21 693 36 67  
E-mail: Hubert.Girault@epfl.ch

[b] Dr. M. Blanchard-Desce  
Département de Chimie  
Ecole Normale Supérieure de Paris, URA CNRS 1679  
24 Rue Lhomond, 75231 Paris Cedex 05 (France)

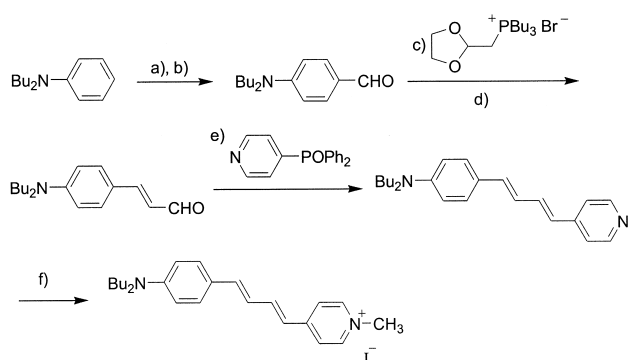
signals, the technique has allowed to probe liquid interfaces with a detailed insight into molecular properties.<sup>[7–9]</sup> At liquid/liquid interfaces, orientation, solvation, and chemical equilibria have been studied<sup>[10, 11]</sup> and polarised interfaces have also been investigated.<sup>[12, 13]</sup> Furthermore, an interfacial polarity scale has been established for a wide range of liquid interfaces with solvatochromic probes.<sup>[14, 15]</sup>

We present in this study a nonlinear spectroscopic investigation of the anion Methyl Orange (MO) at the water/DCE interface in order to understand the solvation environment of the dye and to consequently get an insight into the subsequent electronic reorganisation within the moiety. MO belongs to the family of the *p*-aminoazobenzene derivatives, a family of compounds which have been used in the past to study hydration at protein surfaces as a model to understand the nature of the interaction prevailing in enzyme–substrate associations.<sup>[16]</sup> Second harmonic generation from these compounds has already been reported to have a good efficiency.<sup>[17]</sup>

## Experimental Section

Nonlinear optical measurements were performed with a nanosecond Nd<sup>3+</sup>/YAG laser pumped optical parametric oscillator (OPO). The idler output of the OPO was used at wavelengths ranging from 800 to 1020 nm. Pulses at a repetition rate of 10 Hz with 5 ns duration and energy of 18 mJ were delivered by the laser source. The laser beam was attenuated down to 1 mJ, selectively polarised and focussed onto the water/DCE interface from the DCE phase with an angle of 69.5° to obtain the total internal reflection (TIR) geometry. The TIR configuration indeed greatly enhances the intensity of the SH signal arising from the interface. The SH output from the cell was then separated from the fundamental beam with a filter, collected with a lens, selectively polarised and eventually detected by a photomultiplier tube after wavelength selection through a monochromator. Data were finally acquired with a boxcar integrator. All data were corrected for the wavelength dependence of the laser source power and the acquisition system and the experiments were performed well below the threshold of damages to the surface, ensuring the stability of the interface during the course of the data collection.

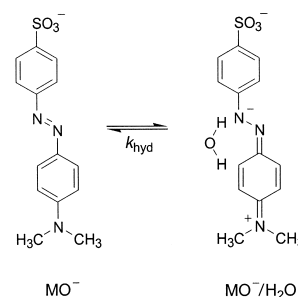
Water was purified by reverse osmosis followed by ion exchange (Millipore, Milli-Q SP reagent system). 1,2-Dichloroethane (DCE) (Merck, extra pure) and sodium Methyl Orange (NaMO) (Aldrich, 95% pure) were used as received. Tetrabutylammonium Methyl Orange (TBAMO) was made by extraction into DCE from an equimolar aqueous mixture of NaMO and tetrabutylammonium chloride (TBACl) (Aldrich) with subsequent solvent evaporation and recrystallisation in acetone. The phase reference dye VA348 was synthesized from *N*-dibutylaniline following a four-step sequence shown in Scheme 1, and characterized by elemental analysis, and mass and NMR spectra.<sup>[18]</sup>



Scheme 1. Synthesis of VA348: a) POCl<sub>3</sub>, DMF; b) H<sub>2</sub>O; c) NaH, THF; d) H<sub>3</sub>O<sup>+</sup>, THF; e) NaH, THF; f) MeI.

## Results and Discussion

**Linear and nonlinear spectroscopy of MO:** *p*-Dimethylaminoazobenzenesulfonate (MO), see structure in Scheme 2, was first studied by UV/Visible spectrophotometry in bulk phases in order to fully resolve its absorption spectrum. In aqueous



Scheme 2. Hydration equilibrium between the hydrogen bonded and the non-hydrogen bonded forms of Methyl Orange.

solutions, the UV/Vis absorption spectrum consists of two bands, see Figure 1, corresponding to two  $\pi-\pi^*$  transitions. The band on the blue side of the spectrum lies at 418 nm and is attributed to the  $\pi-\pi^*$  transition of the nonhydrated moiety, hereafter labelled MO. The band on the red side lies at 467 nm and is attributed to the  $\pi-\pi^*$  transition of the hydrated form MO/H<sub>2</sub>O, which is hydrogen bonded to a water molecule. For the latter form, the presence of the dimethylamino group substituted in *para* position on the end aromatic ring enhances the basicity of the azo group allowing the formation of a hydrogen bond between a water molecule and one of the two nitrogen atoms, see Scheme 2. This bond stabilizes the moiety in polar solvents owing to the resulting charge transfer, yielding a shift to the red of the  $\pi-\pi^*$  transition wavelength. The equilibrium constant  $K_{\text{hyd}} = a(\text{MO}/\text{H}_2\text{O})/a(\text{MO})$  between the hydrated and the nonhydrated forms has been evaluated in the past to be about 100 for 4,4'-diaminoazobenzene, another member of this family of dyes, and closer to unity for MO.<sup>[19, 20]</sup> From the UV/Vis spectra in bulk water for MO concentrations ranging from 5  $\mu\text{M}$  to 10 mM, we determined a value of  $1.2 \pm 0.1$  for the equilibrium constant with a fit to a double Gaussian function. The extinction coefficient of the hydrogen bonded MO/H<sub>2</sub>O form at 467 nm was measured to be  $29700 \text{ M}^{-1} \text{ cm}^{-1}$ . In the bulk DCE phase, the UV/Vis spectrum is markedly different from the bulk aqueous spectrum with the principal band indicative of the non-hydrogen bonded form. The extinction coefficient for the nonhydrated form MO at 418 nm was measured to be  $16500 \text{ M}^{-1} \text{ cm}^{-1}$ . The shoulder at longer wavelengths in the DCE phase, as depicted in Figure 1, shows that the hydrogen-bonded form of the anion MO/H<sub>2</sub>O still coexists in the organic phase, however, with a much lower intensity. This is not surprising since a non-negligible amount of water is present in the DCE phase when the water/DCE interface is at equilibrium. Due to these differences between the UV/Vis absorption spectra in the two media, Methyl Orange is a sensitive probe to study interfacial hydrogen bonding between solutes and water molecules.

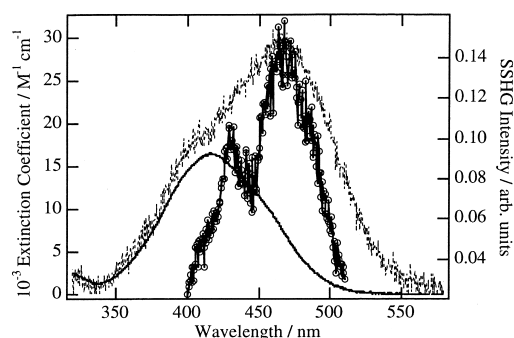


Figure 1. UV/Vis spectra of the aqueous salt NaMO in bulk water (dashed line) and the organic salt TBAMO in bulk DCE (solid line) and surface SH spectrum at the water/DCE interface (open circles).

The surface SH spectrum of MO adsorbed at the water/DCE interface can then be obtained from the wavelength dependence of the SH intensity, with the expression given in Equation (1):<sup>[6]</sup>

$$I^\Omega = \frac{\omega^2}{8 \epsilon_0 c^3 \epsilon_1^\omega (\epsilon_m^\Omega - \epsilon_1^\omega \sin^2 \theta_1^\omega)} \sqrt{\epsilon_1^\Omega} |\chi|^2 (I^\omega)^2 \quad (1)$$

where  $I^\Omega$  is the SH intensity in  $\text{W cm}^{-2}$ ,  $I^\omega$  is the fundamental intensity in the same units,  $\epsilon_1^\omega$  and  $\epsilon_1^\Omega$  are the relative optical dielectric constants of the medium through which the light impinges onto the interface, in this case the organic phase, at the fundamental and the harmonic frequency, respectively,  $\epsilon_m^\Omega$  is the relative optical dielectric constant of the interface at the harmonic frequency and  $\theta_1^\omega$  is the angle of incidence of the fundamental beam. The dielectric constant  $\epsilon_m^\Omega$  was taken as the average of the relative optical dielectric constants of the two bulk phases in line with the recent measurements of the polarity of interfaces.<sup>[14]</sup> Furthermore, all optical dielectric constants were taken as real quantities and without any dispersion relationships. The use of complex dielectric functions to account for the absorptive nature of the aqueous phase was deemed not necessary since the imaginary part was too small to make any significant effect. The same argument holds for the dispersion effect. The quantity  $\chi$  in Equation (1) is defined as:

$$\chi = a_1 \chi_{s,XX}^{(2)} \sin 2\gamma \sin \Gamma + (a_2 \chi_{s,XZX}^{(2)} + a_3 \chi_{s,ZXX}^{(2)} + a_4 \chi_{s,ZZZ}^{(2)}) \cos^2 \gamma \cos \Gamma + a_5 \chi_{s,ZXX}^{(2)} \sin^2 \gamma \cos \Gamma \quad (2)$$

where  $a_i$ ,  $i = 1-5$  are coefficients depending on the relative optical dielectric constants and the angle of incidence  $\theta_1^\omega$ . The angles of polarisation  $\gamma$  and  $\Gamma$  correspond to the fundamental and the harmonic wave, respectively. The tensor elements  $\chi_{s,XZX}^{(2)}$ ,  $\chi_{s,ZXX}^{(2)}$ , and  $\chi_{s,ZZZ}^{(2)}$  are the three nonzero independent elements of the surface susceptibility tensor characterising the nonlinear response of the interface. In the presence of a SHG active monolayer, the contribution to the SH signal of the nearby solvent molecules is negligible, as in the case with the MO dye monolayer, so that the only susceptibility tensor is left for the dye monolayer.<sup>[21]</sup> This macroscopic susceptibility tensor  $\bar{\chi}_s^{(2)}$  may then be related to molecular quantities. It is indeed the product of the total number of optically nonlinear active molecules adsorbed at the interface  $N_s$  and the molecular hyperpolarisability  $\beta$  of a single moiety. For a

monolayer of a mixture of different species, the susceptibility tensor  $\bar{\chi}_s^{(2)}$  is the linear combination of each species susceptibility tensor weighted by its interfacial molar fraction:

$$\bar{\chi}_s^{(2)} = \frac{N_s}{\epsilon_0} (\alpha \langle \bar{\beta}_{\text{MO}/\text{H}_2\text{O}} \rangle + (1-\alpha) \langle \bar{\beta} \rangle) \quad (3)$$

where the brackets around the  $\bar{\beta}$  tensors mean ensemble average over all possible orientation configurations of the adsorbed molecules. In Equation (3),  $\alpha$  is the interfacial mole fraction of the hydrated form MO/H<sub>2</sub>O. The interfacial SH spectrum of the Methyl Orange dye monolayer is shown in Figure 1. It has been measured with both the fundamental and the harmonic waves  $p$ -polarised, that is with  $\gamma = \Gamma = 0^\circ$ . This polarisation configuration yields the largest SH signals, see below and Figure 3. All experiments were conducted in a non-buffered aqueous solution with a pH measured to be about 6.5. Since the  $pK_a$  of Methyl Orange is 3.4, the dye is in its anionic form in water at all times. It is interesting to add that the bulk DCE UV/Vis spectrum of the protonated form of Methyl Orange observed after partitioning from a pH 2 aqueous solution into DCE is similar to the one observed for the anionic form in DCE obtained from the dissolution of the salt TBAMO. This suggests that the protonated form transferred in DCE is the neutral form and not the zwitterionic form. However, at the interface the neutral form is unlikely to exist, as the sulfonate group is likely to reside in the aqueous phase. The MO surface spectrum is closely related to that of the anionic form, since the zwitterionic protonated form has its resonance band located at longer wavelengths. Similar to the UV/Vis spectra, two bands can clearly be seen located at 430 nm and 470 nm; this indicates that both the hydrated MO/H<sub>2</sub>O and the nonhydrated MO forms are present at the water/DCE interface. The band at 430 nm is attributed to the MO form and appears red shifted as compared to the bulk solution. This shift cannot be attributed to an interference effect between the resonant and the non-resonant part of the hyperpolarisability of the MO form. This particular case has been discussed for other compounds and will be discussed in detail below.<sup>[15]</sup> This red shift has already been observed for Methyl Orange in water–organic solvent mixtures and has been discussed in terms of a long range ordering of the aqueous medium with the introduction of a small amount of the organic solvent.<sup>[20]</sup> This can be related to the modifications of the solvent–solvent interactions on the aqueous side of the interface as discussed in molecular dynamics calculations at the water/DCE interface in terms of the strengthening of the hydrogen bonds between water molecules at the interface.<sup>[22]</sup> Hence, the change in the solvent–solvent interaction is reflected in the solute–solvent interaction at the interface provided a sensitive probe is used. Note finally that the low frequency band also shifts towards the red side of the spectrum, however, with a much more reduced shift of only 3 nm, close to the experimental resolution. The overall width of the SH spectrum appears much reduced compared with the linear spectrum, that is about 70 nm against 120 nm for the aqueous linear spectrum, which is a direct result of the nonlinear process. Furthermore, the band located at 470 nm on the SH spectrum is also much larger than its counterpart at 430 nm, a possible result of the rather broad distribution of

the bond distances between the azo group of MO/H<sub>2</sub>O and the hydrogen bonded water molecule. With these results, however, it is not possible to fully determine the hydration equilibrium constant of Methyl Orange at the interface, that is without the ratio of the hyperpolarisability tensors magnitude of the two forms. This question will be addressed below. One conclusion of this first section is that the Methyl Orange principally resides on the aqueous side of the interface since its surface SH spectrum closely resembles the one observed in the bulk aqueous phase by UV/Vis absorption spectroscopy.

**Adsorption isotherm of MO at the water/DCE interface:** The nonlinear optical response of the Methyl Orange monolayer adsorbed at the neat water/DCE interface was monitored as a function of the Methyl Orange aqueous bulk concentration, in order to determine the Methyl Orange adsorption properties. As seen from Equations (1) to (3), the SH response is proportional to the square of the total number of adsorbed molecules,  $N_s$ . Hence, a plot of the square root of the SH intensity against the bulk aqueous concentration of Methyl Orange follows an adsorption isotherm, see Figure 2. In order to probe both Methyl Orange forms, the measurements were conducted for the SH wavelength resonant with the main absorption band of the MO/H<sub>2</sub>O form at 470 nm and the MO form at 430 nm. The bulk aqueous dye concentration was varied from 0 up to 4 mM, although aggregation into dimers and eventually oligomers do occur at higher bulk concentrations. The SH signal was recorded for the fundamental and the harmonic waves both  $p$ -polarized. The isotherm observed on Figure 2 exhibits a simple Langmuir behavior, which indicates that there are no strong interactions between the species present at the interface. Furthermore, from the polarisation dependence at different bulk aqueous dye concentrations it was deduced that local fields could be neglected. At very low concentrations, both isotherms exhibit a linear dependence with the bulk aqueous concentration, as shown in the inset of Figure 2 for the MO/H<sub>2</sub>O form. The flattening of

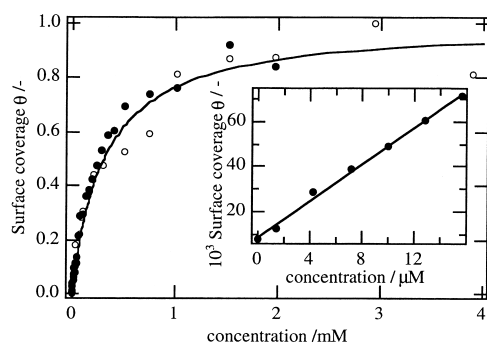


Figure 2. Adsorption isotherm of the non-hydrogen bonded MO form (open circles) and hydrogen bonded MO/H<sub>2</sub>O form (filled circles). The solid line is a fit to a Langmuir adsorption isotherm. The inset shows the adsorption isotherm of the hydrated MO/H<sub>2</sub>O form at very low concentrations.

the isotherm at bulk aqueous concentrations above 1 mM is characteristic of the full monolayer coverage. Unfortunately, no absolute surface density values can be extracted from these measurements by lack of a separate knowledge of the absolute value of the SH intensity and the nonlinear hyper-

polarisability of the dye. The fit of the experimental data to Equation (1) to (3) and a Langmuir isotherm expression is also displayed on Figure 2 and yielded a value of  $-30 \pm 3 \text{ kJ mol}^{-1}$  for the Gibbs energy of adsorption for both the MO/H<sub>2</sub>O and the MO forms. The SH spectrum was also recorded at different surface coverage. However, no change in its general shape was observed, just a mere change in the overall intensity following the isotherm data. Since the bulk aqueous solution equilibrium constant and the adsorption Gibbs energies for both species is known, the surface equilibrium constant can be deduced from a simple thermodynamic cycle between the bulk and the surface; this suggests that the partitioning in the organic phase is negligible. Since both forms have the same Gibbs energy of adsorption, the surface equilibrium constant is about 1.2 and therefore identical to the bulk solution. From this result and the SH spectrum, the ratio of the hyperpolarisability magnitude is close to unity.

Finally, it is worth mentioning that a surface coverage as low as 1% was clearly observed with Methyl Orange. This supports the use of Methyl Orange as an interfacial molecular probe with minimal influence on the surface properties themselves at low coverage. With molecularly engineered compounds with an extremely high nonlinear activity, such as the VA348 compound, coverage as low as 0.01% can easily be detected.

**Orientation of MO at the water/DCE interface:** The orientation of the two forms of MO at the water/DCE interface can be obtained from a light polarisation analysis of the SH intensity. Indeed, and as suggested in Equations (1) and (2), the three susceptibility tensor elements characterizing the Methyl Orange monolayer are determined through measurements as a function of the fundamental wave polarisation angle  $\gamma$  for the SH wave S- ( $\Gamma = 90^\circ$ ) and P- ( $\Gamma = 0^\circ$ ) polarized. In a simple one component monolayer experiment, only one single wavelength measurement would be necessary. However, because the MO monolayer is composed of the two forms of Methyl Orange, see Equation (3), each susceptibility tensor component is the sum of the MO and the MO/H<sub>2</sub>O contribution and therefore the problem requires measurements at several wavelengths. The two forms contribute to the susceptibility tensor elements through their angle of orientation as well as their surface mole fraction and their nonlinear optical activity. The latter quantity is given by the hyperpolarisability tensor that can be reduced to a single non-vanishing element  $\beta_{zzz}$ , that is the component of the tensor along the MO transition moment direction, since the experiments are performed in the vicinity of the  $\pi-\pi^*$  electronic resonance for both forms. Azobenzene dyes are known to have a  $n-\pi^*$  transition in the vicinity of the  $\pi-\pi^*$  one. However, its contribution to the hyperpolarisability tensor is much weaker than the contribution of the  $\pi-\pi^*$  band owing to both a reduced oscillator strength and a reduced charge transfer. The angle of orientation deduced from this analysis refers to the orientation of this transition moment direction with the surface normal. The orientation of the molecule itself at the interface is obtained from the knowledge of the orientation of the transition moment within the molecule but this internal angle is rather small and the transition moment

direction may be taken as identical to the long axis of the molecule. Equation (3) can then be developed for the three non-vanishing susceptibility tensors, yielding:

$$\begin{aligned}\chi_{XZX} = \chi_{ZXX} &= \frac{1}{2\epsilon_0} N_s \beta_{zz,MO} (1 - \alpha_{app}) \langle \cos\theta_{MO} \sin^2\theta_{MO} \rangle \\ &+ \frac{1}{2\epsilon_0} N_s \beta_{zz,MO} \alpha_{app} e^{i\Delta\phi} \langle \cos\theta_{MO/H_2O} \sin^2\theta_{MO/H_2O} \rangle \\ \chi_{ZZZ} &= \frac{1}{\epsilon_0} N_s \beta_{zz,MO} [(1 - \alpha_{app}) \langle \cos^3\theta_{MO} \rangle + \alpha_{app} e^{i\Delta\phi} \langle \cos^3\theta_{MO/H_2O} \rangle]\end{aligned}\quad (4)$$

In Equation (4), the expression is derived without any assumption on the ratio of the  $\beta_{zz}$  element of the two species MO/H<sub>2</sub>O and MO. This implies in particular that the mole fraction  $\alpha_{app}$  is only an apparent mole fraction given by:

$$\alpha_{app} = \frac{\alpha \beta_{zz,MO/H_2O}}{(1 - \alpha) \beta_{zz,MO} + \alpha \beta_{zz,MO/H_2O}} \quad (5)$$

where  $\alpha$  is the true interfacial mole fraction. As mentioned above, since the ratio  $\beta_{zz,MO/H_2O}/\beta_{zz,MO}$  is close to unity, the apparent mole fraction is nearly equal to the true mole fraction. Furthermore, a phase angle between the hyperpolarisability tensor elements of the MO and the MO/H<sub>2</sub>O forms  $\Delta\phi$  has been introduced. Indeed, since the electron density is redistributed within the molecule upon the hydrogen bond formation with the water molecule in the MO/H<sub>2</sub>O form, a phase shift is expected between the two forms. Figure 3 gives the P-curves obtained when the SH intensity is recorded as a function of the fundamental beam polarisation angle at three different wavelengths and different Methyl Orange bulk aqueous concentrations. Only the P-polarised SH curve is given since the S-polarised one does not exhibit any significant change, just a mere overall intensity change. The general form of the S-polarised curve follows a  $\sin^2 2\gamma$  function, see Equations (1) and (2).

The three curves of Figure 3 are normalised with respect to the isotherms presented in Figure 2 and to the Methyl Orange surface spectrum in Figure 1. The molecular parameters obtained from these curves, namely,  $\theta_{MO/H_2O}$ ,  $\theta_{MO}$ , and  $\alpha_{app}$  are given in Table 1. In Figure 3a) is reported the curve obtained with the SH wavelength set at 507 nm. This wavelength corresponds to a fundamental wavelength of 1014 nm and the Methyl Orange bulk aqueous concentration was set at 3  $\mu\text{M}$ . This low bulk concentration ensured that the curve was recorded at a very low surface coverage where interactions between neighboring Methyl Orange species at the interface are minimized. From the isotherm, the corresponding surface coverage is estimated to be 2%. The SH wavelength of 507 nm was chosen to yield measurements with the hydrated MO/H<sub>2</sub>O form only, as the MO form transition band is located far away to the blue at 430 nm. Hence, the polarisation curve can be taken as the one of pure MO/H<sub>2</sub>O and Equation (4) allows the determination the MO/H<sub>2</sub>O transition moment angle of orientation unambiguously. This angle of orientation of the transition dipole moment was found to be  $43 \pm 2^\circ$  with respect to the surface normal, assuming an infinitely sharp distribution. This latter assumption underlines the character of this angle which defines the angle distribution but does not give the real tilt angle of the adsorbed dye molecules at the

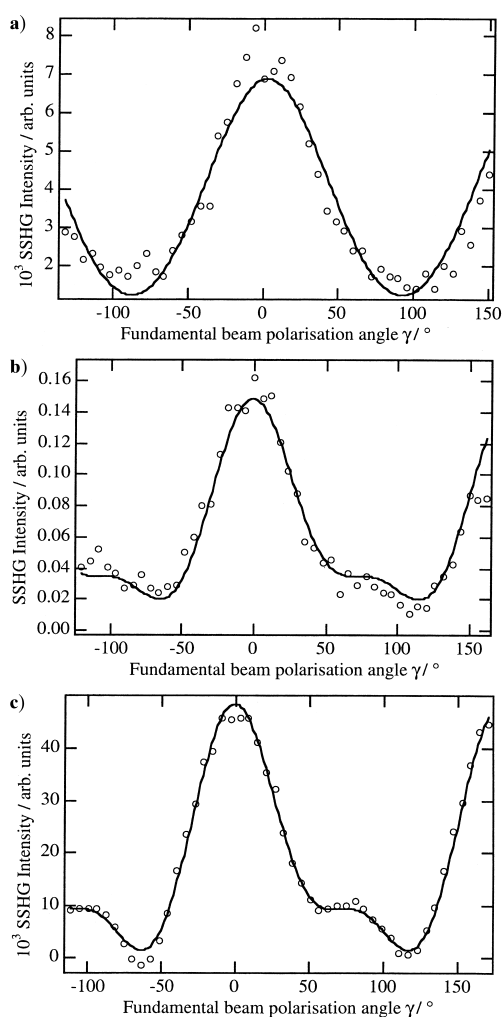


Figure 3. Polarisation curves for different MO concentrations and harmonic wavelengths: a) 3  $\mu\text{M}$ , 507 nm; b) 30  $\mu\text{M}$ , 470 nm; c) 1 mM, 387 nm. The harmonic beam is P-polarised. The solid lines are fits obtained using Equations (1) to (5).

Table 1. Molecular parameters obtained for the hydrated MO/H<sub>2</sub>O and the nonhydrated form MO of Methyl Orange at the water/DCE interface.

	MO/H <sub>2</sub> O	MO
$\theta$ [°]	43	34
$\beta^{NR}$	-0.44	0.0054
$A$	$-5.9 \times 10^{-7}$	$3.1 \times 10^{-7}$
$\omega$ [nm]	470	430
$\alpha_{app}$	0.5	0.5

interface. The absolute orientation can not be measured with this experiment, but it is reasonable to assume that the sulfonate polar head points towards the aqueous side of the interface. The polarisation curve in Figure 3b) was then measured at a Methyl Orange bulk aqueous concentration of 30  $\mu\text{M}$  corresponding to a still rather low surface coverage of about 15% where solute-solute interfacial interactions are rather weak, and a SH wavelength of 470 nm. At this wavelength, the measured SH signal contains an overwhelming contribution from the MO/H<sub>2</sub>O form, but a non-negligible contribution from the MO form leads to the observed

distorted shape of the polarisation curve. It is to be pointed out that these measurements were performed with an achromatic half-wave plate in order to avoid any improper polarisation rotation. Keeping the MO/H<sub>2</sub>O angle of orientation deduced above as a constant parameter, the MO angle of orientation of the transition moment can then be determined, which is found to be  $34 \pm 2^\circ$  with respect to the surface normal. This procedure was repeated at several other wavelengths, for example at 387 nm, see Figure 3c), where the dominant contribution arises from the MO form and yielded a similar value. The transition dipole moment of the MO/H<sub>2</sub>O has thus the tendency to lie flatter at the water/DCE interface than that of the MO form. The apparent mole fraction of the MO/H<sub>2</sub>O form,  $\alpha_{\text{app}}$ , also determined from the polarisation curve, was found to be 0.5. This value is in agreement with the value of 0.55 corresponding to the equilibrium constant of about 1.2. The surface hydration equilibrium constant between the two Methyl Orange forms at the neat water/DCE interface is therefore the same as in bulk water. The last parameter determined from the fit of the polarisation curves is the phase shift between the two hyperpolarisability tensor elements of the MO and of the MO/H<sub>2</sub>O forms. This phase shift  $\Delta\phi$  was found to be weakly dependent with the wavelength and equal to  $206^\circ$ . It was, however, noted that rather good fitted curves could be obtained with a wide range of values for this phase shift  $\Delta\phi$ , but that these values always fell between  $120^\circ$  and  $240^\circ$ . This observation of a constant phase shift is rather surprising as this angle should have been evolving along the spectrum in this wavelength region that corresponds to the neighborhood of the resonance. This is the normal expectation for a single adsorbed compound, the phase evolving by  $180^\circ$  across the resonance, its value being exactly  $90^\circ$  at the resonance. The weak wavelength dependence of the  $\Delta\phi$  parameter is, however, explained by the interference pattern between the two forms of Methyl Orange and the presence of a significant non-resonant contribution to the hyperpolarisability tensor. Indeed, the value of  $206^\circ$  suggests that the two forms of MO have an opposite direction, one pointing up and the other down. Furthermore, the non-resonant contribution to the hyperpolarisability tensor is rather independent of the wavelength. Thus, the overall phase shift  $\Delta\phi$  is the difference in the two phase shifts which partially compensate along the spectrum yielding this independent behavior as a function of wavelength, provided the sulfonate hydrophilic group constantly points into the aqueous phase.

The phase shift of  $180^\circ$  between the two tensor elements for the two Methyl Orange forms implies an electronic reorganisation within the molecule subsequent to the hydrogen bond formation. A simple picture can be proposed within the framework of the two-level two-state model.<sup>[23]</sup> For compounds undergoing a rather large charge transfer upon excitation, the fundamental  $|\psi_g\rangle$  and the excited  $|\psi_e\rangle$  states can be taken as a superposition of a neutral  $|N\rangle$  and a zwitterionic  $|Z\rangle$  form. This is usually written as:<sup>[23]</sup>

$$\begin{aligned} |\psi_g\rangle &= \cos\frac{\theta}{2}|N\rangle + \sin\frac{\theta}{2}|Z\rangle \\ |\psi_e\rangle &= -\sin\frac{\theta}{2}|N\rangle + \cos\frac{\theta}{2}|Z\rangle \end{aligned} \quad (6)$$

where the angle  $\theta$ , taken between 0 and  $\pi$ , defines the weighted contributions of the neutral and the zwitterionic forms in the ground and the excited state. In this framework, the neutral form is the basic electronic structure where no charge transfer has taken place whereas the zwitterionic one is the one obtained after that full charge transfer has occurred. In the case of the dye Methyl Orange, the two forms *N* and *Z* are shown on Figure 4 for the hydrated and the nonhydrated forms. The nonhydrated MO form is a classical push–pull type compound with a donor group, the dimethylamino moiety, and an acceptor group, the sulfonate group, well separated by an extensive  $\pi$ -electron system.

The neutral form is therefore the basic electronic structure, whereas the zwitterionic form  $Z_{\text{MO}}$  is obtained with a charge transfer from the donor amino group to the acceptor sulfonate group, along the full length of the molecular long axis. In the case of MO, the neutral form has a dominant contribution to the description of the ground state structure (i.e.,  $0 < \theta < \pi/2$ ) due to the large aromatic stabilisation brought by the two phenyl rings and the high energetic cost associated with the charge separation over the total length of the molecule. The context is different for the hydrated form for which different *N* and *Z* forms can be proposed due to the presence of the hydrogen bond. The neutral form is the basic structure with the hydrogen bond formed. The charge transfer from the dimethylamino donor to the now azo group acceptor yields a different zwitterionic form  $Z_{\text{MO/H}_2\text{O}}$ , which is strongly stabilized by hydrogen bonding and involves less aromatic stabilisation loss and shorter charge separation than  $Z_{\text{MO}}$ . Due to the relative stabilisation of the *Z* form with respect to the *N* form brought by the hydrogen bonding, one could expect a dominant contribution of the *Z* form in the case of the hydrated form MO/H<sub>2</sub>O (i.e.,  $\pi/2 < \theta < \pi$ ). This is expected to lead to opposite sign of  $\beta$ .<sup>[23]</sup> The distance along which the charge transfer occurs being different and the mixing element between the neutral and the zwitterionic forms being not strictly opposite, it is possible that the phase shift between the two MO forms does not exactly equal  $\pi$ . Hence, an electron density redistribution upon the hydrogen bond formation is experimentally observed through the interference of the two hyperpolarisability elements as exhibited by the phase angle  $\Delta\phi$  of about  $206^\circ$  between the two forms MO and MO/H<sub>2</sub>O in the light polarisation data.

**Phase interference between MO and MO/H<sub>2</sub>O:** In order to further evidence the phase inversion of the hyperpolarisability tensor element between MO and MO/H<sub>2</sub>O, the SH spectrum of these two species was recorded in the presence

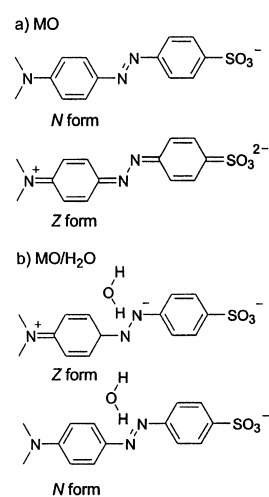


Figure 4. Neutral (*N*) and zwitterionic (*Z*) forms of nonhydrated a) and hydrated b) Methyl Orange within the two-state two-level model.

of a third compound, see Figure 5. This VA348 compound is another push–pull type molecule with a very high nonlinear optical activity whose main electronic transition lies around 579 nm in dichloromethane. This compound is thus used as a reference phase for the two forms of Methyl Orange since it is expected that its phase evolution with the wavelength is

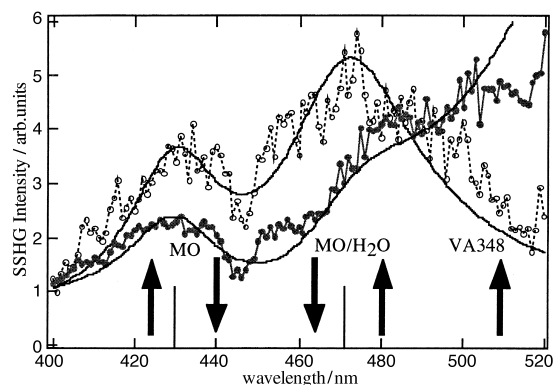


Figure 5. Surface SHG spectra of the hydrated MO/H<sub>2</sub>O and dehydrated MO forms of Methyl Orange adsorbed at the water/DCE interface (open circles) and of a mixed monolayer of Methyl Orange and VA348 (filled circles). The solid lines are simulated curves obtained with the data given in Table 1. Arrows give the region of constructive (arrows up) and destructive (arrows down) interference.

smooth enough in the range 400 to 500 nm. To perform this measurement, the Methyl Orange dye was first dissolved in the organic phase as a tetrabutylammonium salt since the VA348 is not soluble in the aqueous phase.

It is to be noted that the observed surface SH spectrum of the Methyl Orange organic salt was identical to the one reported on Figure 1; this indicates that the surface solvation properties of Methyl Orange were independent of the phase from where it was adsorbing. The spectrum obtained in the presence of a small amount of VA348 clearly shows that on the red side of the resonance of MO/H<sub>2</sub>O a constructive interference occurs, as exhibited by the sharp increase in intensity. On this side of the spectrum, MO/H<sub>2</sub>O and VA348 have thus similar phases. This is exactly what is expected since VA348 is a classical push–pull molecule, with a behavior similar to the nonhydrated form MO. In particular it is expected that its donor group, the dibutylamino end will point into the organic phase just as the dimethylamino end group of MO points into the organic phase. On the red side of the MO/H<sub>2</sub>O resonance, and therefore the blue side of the VA348 resonance, these two compounds have constructive phases, see Figure 5. On the blue side of the 470 nm resonance, a clear drop in intensity is observed indicating a destructive interference in accordance with the flip of the MO/H<sub>2</sub>O phase across the resonance. A similar destructive pattern occurs on the red side of the 430 nm resonance. This implies as expected that the MO form is phase shifted as compared to VA348 in this region since this corresponds to the blue side of the VA348 resonance and the red side of the MO resonance. On the blue side of the 430 nm band, however, the interference is constructive again but the effect tends to vanish as the wavelength range is now more than 100 nm away from the

VA348 resonance. The general phase interference pattern is therefore inverted for the two MO and MO/H<sub>2</sub>O forms, as schematically shown on Figure 6, but similar for the MO and the VA348 compounds. This inversion of phase clearly emphasizes the electron density redistribution that occurred in the Methyl Orange moiety upon the hydrogen bond formation.

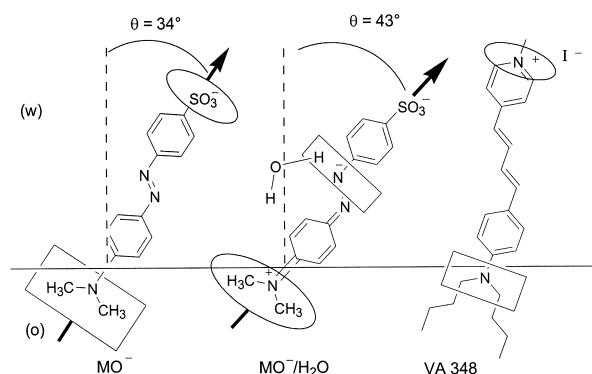


Figure 6. Schematic of the orientation of the two forms of Methyl Orange and the absolute orientation of VA348 at the water/DCE interface. Donor groups are underlined by rectangles and acceptor groups by ellipses.

The SH spectra with and without the VA348 phase reference were also simulated using Equation (1) to (5) extended to take into account the VA348 contribution. The wavelength dependence of the  $\beta_{zzz}$  elements was described within the two-level model as:

$$\beta_{MO} = \beta_{MO}^{NR} + \frac{A_{MO}}{[\omega_{0,MO}^2 - 4\omega^2 - 4i\gamma_{MO}\omega]} \quad (7)$$

$$\beta_{MO/H_2O} = \beta_{MO/H_2O}^{NR} + \frac{A_{MO/H_2O}}{[\omega_{0,MO/H_2O}^2 - 4\omega^2 - 4i\gamma_{MO/H_2O}\omega]}$$

where  $\beta_{MO}^{NR}$  and  $\beta_{MO/H_2O}^{NR}$  are the non-resonant part of the molecular hyperpolarisability tensor,  $A_{MO}$  and  $A_{MO/H_2O}$  are two constants,  $\omega_{0,MO}$  and  $\omega_{0,MO/H_2O}$  are the transition frequencies and  $\gamma_{MO}$  and  $\gamma_{MO/H_2O}$  the damping constants. To account for the opposition of the transition moments,  $\beta_{MO/H_2O}$  was set to a negative value, whereas  $\beta_{MO}$  and  $\beta_{VA348}$  were set positive. In these calculations, the orientation angles found in the light polarisation analysis were used and the spectrum without the VA348 contribution, similar to the one shown on Figure 1, was simply obtained by setting the  $\beta_{VA348}$  tensor to zero, keeping all the two MO forms parameters untouched. All the microscopic data used are reported in Table 1. It is important to note though that the width of the resonance deduced from the fitting procedure accounts for the inhomogeneous broadening as a result of the use of the macroscopic susceptibility tensor. This is not a microscopic parameter and therefore does not appear in Table 1. As can be seen in Figure 5, the simulated curves are in good agreement with the experimental data. One interesting feature obtained from the data is the rather strong contribution arising from the non-resonant background of the hydrated form of Methyl Orange as compared to the nonhydrated form. Figure 6 gives a schematic of the different orientation of the compounds at the interface.

## Conclusion

The interfacial properties of hydration of the dye Methyl Orange have been studied at the neat water/DCE interface. We found that a simple Langmuir isotherm with a Gibbs energy of adsorption of about  $-30 \text{ kJ mol}^{-1}$  could describe correctly the interfacial adsorption of both the hydrated MO/H<sub>2</sub>O and the nonhydrated MO forms at the neat water DCE interface. This suggests in turn a surface hydration equilibrium identical to the bulk aqueous phase one. Furthermore, it is noted that the hydrated form of MO/H<sub>2</sub>O is found to lie flatter at the interface. From the light polarisation analysis, and more interestingly, from a phase interference with a third compound used as an internal phase reference, an intramolecular electron density redistribution is clearly observed. Upon the hydrogen bond formation with a water molecule, a complete flip of the phase of the hyperpolarisability tensor has occurred within the dye compound. The interference pattern underlines the sensitivity of surface nonlinear spectroscopy to the direct investigation of intramolecular electronic rearrangements within molecules at interfaces resulting from the interactions with the solvent.

## Acknowledgements

The authors would like to thank fruitful discussions with Prof. R. M. Corn at the beginning of this work. The support of the Fonds National Suisse de la Recherche Scientifique under grant No. 2000-043381.95/1 is kindly acknowledged. J.R. acknowledges the Ecole Polytechnique Fédérale de Lausanne for a research fellowship. The Laboratoire d'Electrochimie is part of the European Training and Mobility of Researchers network "Organisation, Dynamics and Reactivity at Electrified Liquid/Liquid Interfaces (ODRELLI)".

- [1] R. L. Reeves, S. A. Harkaway, *J. Colloids Interf. Sc.* **1978**, *64*, 342.
- [2] J. M. Perera, G. W. Stevens, F. Grieser, *Colloids Surf. A* **1995**, *95*, 185.
- [3] H. Watarai, Y. Saitoh, *Chem. Lett.* **1995**, 283.
- [4] R. A. W. Dryfe, Z. Ding, R. G. Wellington, P. F. Brevet, A. M. Kuznetsov, H. H. Girault, *J. Phys. Chem.* **1997**, *101*, 2519.
- [5] Y. R. Shen, *The principles of nonlinear optics*, Wiley, NY, **1984**.
- [6] P. F. Brevet, *Surface second harmonic generation*, Presses polytechniques et universitaires romandes, Lausanne, **1997**.
- [7] P. F. Brevet, H. H. Girault in *Liquid-Liquid Interfaces: Theory and Methods* (Eds.: A. G. Volkov, D. W. Deamer), CRC Press, Boca Raton, **1996**, p. 103.
- [8] R. M. Corn, D. A. Higgins, *Chem. Rev.* **1994**, *94*, 107.
- [9] K. B. Eisenthal, *Chem. Rev.* **1996**, *96*, 1343.
- [10] A. A. Tamburello-Luca, P. Hébert, P. F. Brevet, H. H. Girault, *J. Chem. Soc. Faraday Trans.* **1996**, *92*, 3079.
- [11] X. D. Xiao, V. Vogel, Y. R. Shen, *Chem. Phys. Lett.* **1989**, *163*, 555.
- [12] R. R. Naujok, D. A. Higgins, D. G. Hanken, R. M. Corn, *J. Chem. Soc. Faraday Trans.* **1995**, *91*, 1411.
- [13] R. R. Naujok, H. J. Paul, R. M. Corn, *J. Phys. Chem.* **1996**, *25*, 10497.
- [14] H. F. Wang, E. Borguet, K. B. Eisenthal, *J. Phys. Chem. A* **1997**, *101*, 713.
- [15] H. Wang, E. Borguet, K. B. Eisenthal, *J. Phys. Chem. B* **1998**, *102*, 4927.
- [16] I. M. Klotz, R. K. Burkhard, J. M. Urquhart, *J. Am. Chem. Soc.* **1952**, *74*, 202.
- [17] A. K. Kakkar, S. Yitzchaik, S. B. Roscoe, T. J. Marks, W. P. Lin, G. K. Wong, *Thin Solid Films* **1994**, *242*, 142.
- [18] V. Alain, M. Blanchard-Desce, unpublished results.
- [19] W. R. Brode, I. L. Seldin, P. E. Spoerri, G. M. Wyman, *J. Am. Chem. Soc.* **1955**, *77*, 2762.
- [20] R. L. Reeves, R. S. Kaiser, M. S. Maggio, E. A. Sylvestre, W. H. Lawton, *Can. J. Chem.* **1973**, *51*, 628.
- [21] A. A. Tamburello-Luca, P. Hébert, P. F. Brevet, H. H. Girault, *J. Chem. Soc. Faraday Trans.* **1995**, *91*, 1763.
- [22] I. Benja min, *J. Chem. Phys.* **1992**, *97*, 1432.
- [23] M. Blanchard-Desce, M. Barzoukas, *J. Opt. Soc. Am. B* **1998**, *15*, 302.

Received: October 11, 1999

Revised version: December 23, 1999 [F2079]